

Modelling Non-Invasive Ultrasonic Tomography for Industrial Liquid/Gas Flow Application

¹Fazalul Rahiman M.H., ²Abdul Rahim R., ³Fazalul Rahiman M.H. and ¹Tajjudin M.

¹Mechatronic Engineering Department, Faculty of Engineering,
Universiti Industri Selangor, 40000 Shah Alam, Selangor, Malaysia.
hafizfr@yahoo.com

²Process Tomography Research Group (PROTOM), Control and Instrumentation Engineering
Department, Faculty of Electrical Engineering, Universiti Teknologi Malaysia, 81310 Skudai, Johor,
Malaysia. ruzairi@fke.utm.my

³Faculty of Electrical Engineering, Universiti Teknologi MARA, 40450 Shah Alam, Malaysia.
hezrif@ieee.org

Abstract

This paper presents modelling of non-invasive Ultrasonic Tomography via transmission-mode method for imaging liquid and gas flow. Transmission-mode approach has been used for sensing the liquid/gas two-phase flow, which is a kind of strongly inhomogeneous medium. The concept of observation time and the imaging technique for two-phase flow using fan-shaped beam scanning geometry were presented.

Keywords: Acoustic Imaging, Fluid Flow Measurement, Image Reconstruction, Ultrasonic Modelling.

1. Introduction

The measurement of two-component flow such as liquid or oil flow through a pipe is increasingly important in a wide range of applications, for example pipeline control in oil exploitation and chemical process monitoring. Knowledge of the flow component distribution is required for the determination of flow parameters such as the void fraction and the flow regime. Real-time reconstruction of the flow image is needed in order to estimate the flow regime when it is continuously evolving. Real time process monitoring plays a dominant role in many areas of industry and scientific research concerning liquid/gas two-phase flow. It is proved that the operation efficiency of such a process is closely related to accurate measurement and control of hydrodynamic parameters such as flow regime and flow rate [1]. Besides, monitoring in the process industry has been limited to either visual inspection or single point product sampling where product uniformity is assumed. This approach for the determination of fluid flow parameters of two-component flow is called flow imaging.

2. Ultrasonic Attenuation Model

The attenuation process may be modelled by Lambert's exponential law of absorption [2], where the ultrasonic energy intensity of transmitter and receiver are related as in Figure 1 (where L represents the total path length):

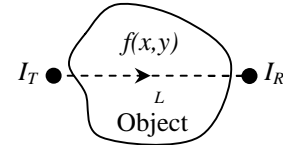


Figure 1: The ultrasonic attenuation model.

$$I_R = I_T \exp\left(-\int_L f(x, y) dl\right) \quad (1.1)$$

where

I_R = the receiver intensity

I_T = the transmitter intensity

L = path length in the object field

$f(x, y)$ = the attenuation function by the object field

As introduced above, the attenuation will critically depend upon the material through which the ultrasound travels. Thus, attenuation model for ultrasonic transducer can be simplified as in Figure 2.

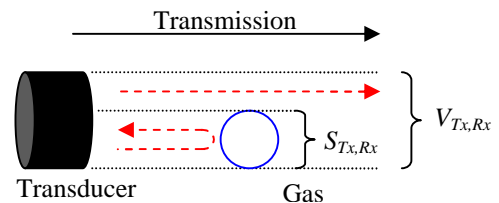


Figure 2: The attenuation model for ultrasonic transmitter.

The ultrasonic receiver voltage (sensor value) is represented by $V_{Tx,Rx}$ and the sensor loss voltage due

to the gas cavity is represented by $S_{Tx,Rx}$. The sensor loss voltage increases proportionally according to size of gas cavity as the gas cavity blocks the ultrasound energy transmitted to the receiver. Therefore the receiver voltage (sensor value) is decreased as the sensor loss voltage increased. In figure 2, the transmitted signal is reflected on the liquid/gas interface. At room temperature, both water (liquid) and air (gas) have acoustic impedance of $1.5 \times 10^6 \text{ kg/m}^2\text{s}$ and $430 \text{ kg/m}^2\text{s}$ respectively. The reflection coefficient, R at the interfaces can be calculated as below:

$$\begin{aligned} R_{(liquid / gas)} &= \left[\frac{Z_2 - Z_1}{Z_2 + Z_1} \right] \\ &= \left[\frac{430 - 1.5 \times 10^6}{430 + 1.5 \times 10^6} \right] \\ &= -0.9994 \Rightarrow -99.94\% \end{aligned} \quad (1.2)$$

where

Z_1 = the liquid (water) acoustic impedance ($\text{kg/m}^2\text{s}$)

Z_2 = the gas (air) acoustic impedance ($\text{kg/m}^2\text{s}$)

The negative sign indicates the reversal of the phase relative to the incident wave. In above calculation, it shows that due to the large different of acoustic impedance between the liquid and gas medium, therefore 99.94% of ultrasonic wave will be reflected at liquid/gas boundary and scattered within the liquid area

3. Ultrasonic Transmission-Mode Modelling

Ultrasonic imaging relies on the measurement of the transmitted and/or reflected ultrasonic wave. The received amplitude and phase characteristics of reflected ultrasound are critically dependent on the object shape, orientation and position in relation to the transmitter and receiver geometry. Therefore, reflection-mode measurement schemes are generally more demanding in terms of complexity and transducer performance [3]. The system presented here utilized transmission-mode measurement of transmitted signal amplitude. The modelling of the system is described in the following.

The ultrasonic sensing model has been reduced to two dimensions with fan-shaped beam profiles on the assumption that the ultrasonic wave propagates in a straight line [11]. Due to significant of acoustic impedance mismatch between the two components of liquid and gas flow, ultrasound incident wave on a boundary between components will be totally reflected [4]. The gas hold-ups in the measurement section should be greater than at least half of the ultrasonic wavelength to block the ultrasonic energy from reaches the receiver during the measurement period [3, 4]. The significant relationship for the ultrasonic wavelength is shown as below:

$$n = fl \quad (1.3)$$

where

v = speed of sound (m/s)

f = ultrasonic frequency (Hz)

l = the wavelength (m)

In this system, a 40kHz transducer frequency, (f) is chosen and it is known that the speed of sound, (v) in water at 25°C is 1500m/s. Thus, the ultrasonic wavelength obtained is 38mm. From the previous quotation, the resolution for the transducer was set to half-wavelength. Therefore, the resulting resolution is 19mm. Therefore, the gas hold-up size or the gas bubbles should be at least 19mm in diameter so that it could be sensed by the ultrasonic sensing array.

Figure 3 shows the transmitter with a fan-shaped beam transmission. The transmitter is modelled as a point source which propagates within angle α in the image plane and the receiver is modelled as a circular arc with radius of curvature r . The wavefronts are taken to be circular arcs of uniform ultrasonic energy. When ultrasound is propagating in the flow medium, areas occupied by the discontinuous component block the transmitted ultrasound [5]. As a result, an effect analogous to the shadowing of visible light by an opaque object can be seen in Figure 3. An example of transmitted ultrasonic signal and received ultrasonic signal is shown in Figure 4.

This paper proposed a transmission-mode method emphasizing the receiver amplitude and the arrival time analysis. Arrival time analysis is based on the simple fact that it takes some finite time for an ultrasonic disturbance to move from one position to another inside the experimental pipe. In Figure 4, the *observation time* denoted by t_s was the first peak after the time-of-flight corresponding to a straight path. By sampling amplitude of this observation time for every receiving sensor due to projection of transmitters, the information via transmission-mode method can be obtained [1]. As the distance between the transmitting sensor and the receiving sensor increases, the ultrasound will consume longer time-of flight to reach to the point of interest and therefore set out a longer observation time. This time-of-flight may then be assumed to be proportional to the distance that they had travelled [6, 7].

Basically, the ultrasonic beam by the longitudinal waves could penetrate through the pipe from the transmitting sensor to the receiving sensor within a low acoustic impedance media such as liquid. For example, the penetration of longitudinal waves from the transmitting sensor of Tx13 to the receiving sensor of Rx4 is shown in Figure 5. However, there is another wave generated due the complex vibrational effects known as the Lamb waves. The Lamb waves is a wave that propagates and travels within the pipe boundary and it is shown in Figure 6. Transmission-mode method requires that, the amplitude of observation time should be obtained

from the longitudinal waves and not the Lamb waves. This is because the lamb wave propagates within the pipe boundary and the observation time obtained from

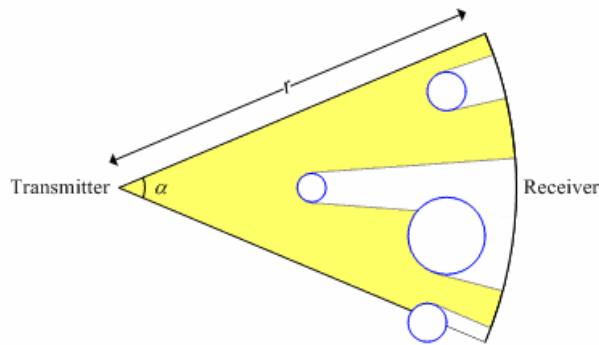


Figure 3: Transmission-mode with fan-shape beam transmitter projection.

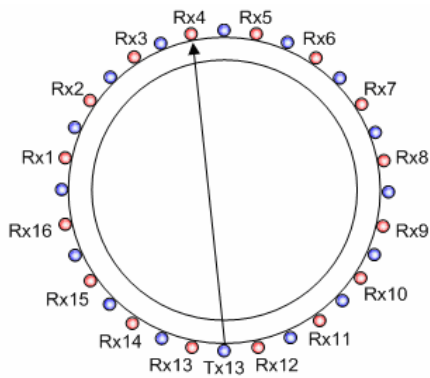


Figure 5: Penetration by the longitudinal wave from Tx13 to Rx4.

Obviously shown in Figure 5 and Figure 6, the distance of ultrasonic penetration by the longitudinal wave from Tx13 to Rx4 is shorter, compared to the distance of Lamb wave propagation from Tx13 to Rx4. To verify this, a case study needs to carry out. A projection from Tx13 is generated and by using a calibrated Tektronix Digital Oscilloscope TDS3012, the ultrasound time-of-flight (TOF) for simulation of three static conditions of full liquid flow, half liquid flow and zero liquid flow were determined. Water has been used as the liquid media. The time-of-flight obtained for every receiving sensors covered by transmitter Tx13 divergence's angle are tabulated in Table 1. Data from the Table 1 is represented as graph in Figure 7.

During full liquid flow, the pipe will wholly occupied by the liquid. The liquid already provide low acoustic impedance and therefore the penetration of longitudinal waves to every receiving sensor are successful and the time-of-flights obtained are as tabulated in Table 1. During half liquid flow the gas phase flows in the upper section and the liquid in the

the Lamb waves does not provide any information of ultrasonic disturbances caused by the gas obstruction in the pipe.

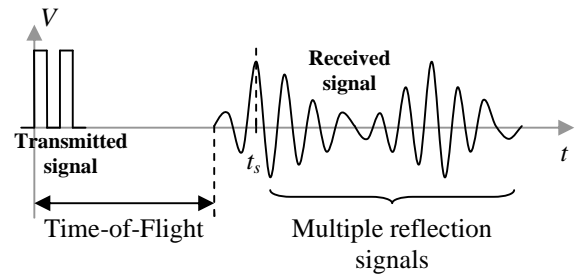


Figure 4: Example of a transmitted and a received signal.

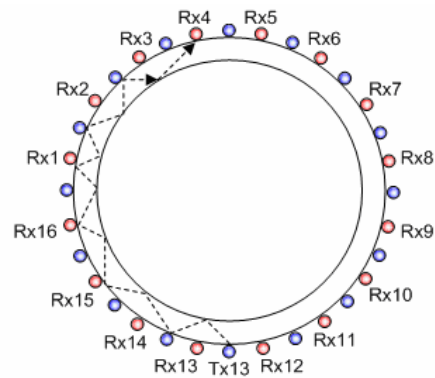


Figure 6: The Lamb wave propagation from Tx13 to Rx4.

lower section. As a result, only receiver Rx16 and Rx9 will received the longitudinal waves from Tx13 and for the rest of receivers, the longitudinal waves will be reflected at the liquid and gas boundary because of both yield high acoustic impedance and this is shown in Figure 8. For zero liquid flow, the gas phase will be occupied in the whole section, thus creating a high acoustic impedance region which rejects the longitudinal waves from being transmitted. All of the receiving sensors therefore will receive the lamb waves instead of the longitudinal waves. The Lamb wave's time-of-flight should be longer and this is shown in Table 1.

From the case study above, it is found that the time of observation, (t_s) that lies on the first arrival of the received ultrasonic wave (by the longitudinal wave) is absolutely free from being fused by the Lamb waves. Thus, the propagation of Lamb waves is negligible and discarded in the modelling. The method of making use the observation time will be described for the rest of this sub-section.

Table 1: The time-of-flight (TOF) due to projection Tx13.

Projection	Full Flow (TOF)	Half Flow (TOF)	Zero Flow (TOF)
Tx13 – Rx16	54.4 μs	54.4 μs	59.2 μs
Tx13 – Rx1	62.4 μs	74.0 μs	74.0 μs
Tx13 – Rx2	73.8 μs	94.4 μs	94.4 μs
Tx13 – Rx3	76.4 μs	118.0 μs	118.0 μs
Tx13 – Rx4	77.8 μs	128.0 μs	128.0 μs
Tx13 – Rx5	78.0 μs	128.4 μs	128.4 μs
Tx13 – Rx6	75.8 μs	117.8 μs	117.8 μs
Tx13 – Rx7	68.6 μs	94.4 μs	94.4 μs
Tx13 – Rx8	66.0 μs	73.8 μs	73.8 μs
Tx13 – Rx9	50.6 μs	50.6 μs	59.0 μs

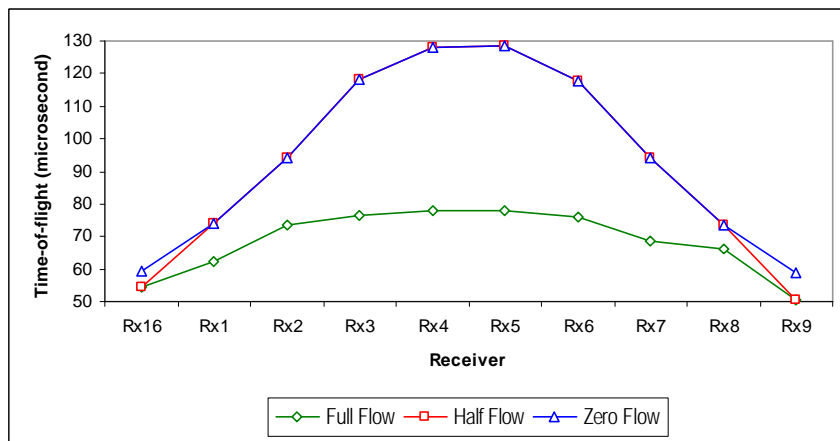


Figure 7: The graph for time-of-flight due to projection Tx13.

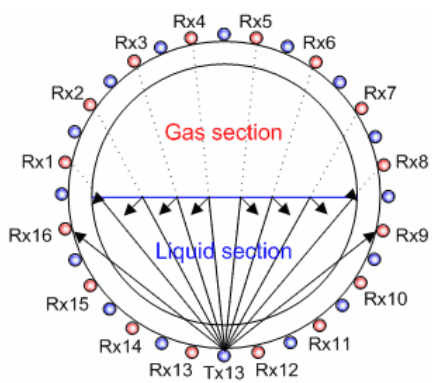


Figure 8: Simulation of projection Tx13 during half liquid flow.

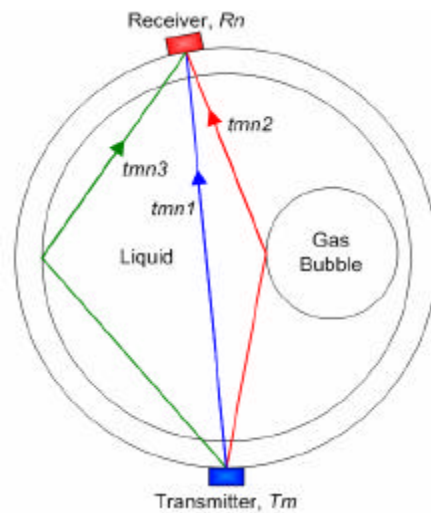


Figure 9: Three possible paths for receiving signals.

In Figure 4, the observation time denoted by t_s was the first peak of the time-of-flight signal corresponds to a straight path. When the components to be imaged are gas, there may be no directly transmitted signals from the transmitter to the receiver because of the obstacles. By reflecting against the pipe wall or multiple reflections on the gas component surfaces, the receiver may still detect some signals but at later time though because direct transmission takes the shortest path and hence the shortest time. Thus, if the observation time is monitored, it is easy to test whether there are any objects between the transmitter and the receiver. This concept of transmission-mode has been used within this paper. Figure 9 shows three possible paths for the receiving signals.

We noticed that the receiving signals may come from the direct transmission (t_{mn1}), the reflected signals by gas component surfaces (t_{mn2}) and the reflected signals against the pipe wall (t_{mn3}). If we take Figure 9 as an example, we found that the shortest path will provide the shortest observation time that is t_{mn1} . The reflected signals, t_{mn2} and t_{mn3} however will arrive later. The delay between each receiving signals are represented as in Figure 10.

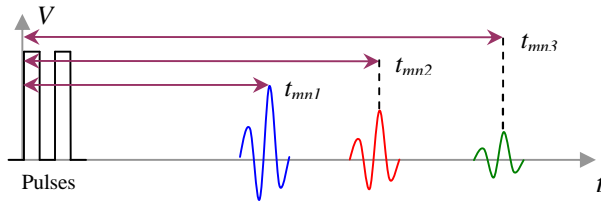


Figure 10: Receiving signals for different sound paths.

When a pulse is transmitted from the transmitter, for each receiver there is a specific observation time at which the transmitted pulse should arrive. This time is the shortest time and the path between the transmitter and receiver is a straight line. These observation times are therefore used for calibrating the measurement section. By using a calibrated Tektronix Digital Oscilloscope, TDS3012 the observation times for each receiver is recorded and then programmed into the microcontroller.

4. Multi-Fluid Flow System

Although the designation and the experiment carried out for this system applied to water, it is also expected suitable for different types of liquid such as oils and chemical liquids as well. The different between those liquids is only the density and the viscosity [8]. Highly viscous fluid generally has associated with them high levels of attenuation of ultrasound. So for example, water has a kinematics viscosity of $1.003 \times 10^{-6} \text{m}^2 \text{s}^{-1}$ at 25°C and attenuation at 1MHz of a pressure wave of 0.22dB/m whereas a product such as castor oil has kinematics viscosity of $1.1 \times 10^{-2} \text{m}^2 \text{s}^{-1}$ and an attenuation of 95dB/m at 1 MHz [9]. This different affects the observation time

which by means the speed of sound in the corresponding liquids. Thus, the observation times for those liquid is needed if it is necessitate for flow imaging.

5. Fan-Shaped Beam Projection Geometry

The transducer configuration is a key factor in the efficiency of data acquisition; it has both static and dynamic characteristics [10]. The static characteristics are the fundamental parameters which determine the physical structure of the configuration. This system employs 16 pairs of ultrasonic transducer with 8.2mm in diameter for each transducer. Both ultrasonic transmitters (Tx1-Tx16) and receivers (Rx1-Rx16) have a divergence angle, $\alpha = 125^\circ$ and were arranged around the circumference of the experimental pipe. The experimental pipe was acrylic type with 103mm inner diameter and 6mm thickness. By using the transmission-mode method and the fan-shaped beam projection technique, the ultrasonic transmitters will transmit pulses at 40 kHz through the experimental vessel to the point of interest. Each transmitter excited will emit two cycles of tone burst of 40kHz at 20Vp-p and each projection from the transmitting transducers will cover up to 10-channels of the receiving transducers. A total of 16 projections were made in one scan, hence 160 independent measurements were obtained. Figure 11 and Figure 12 show the scanning geometry for the system.

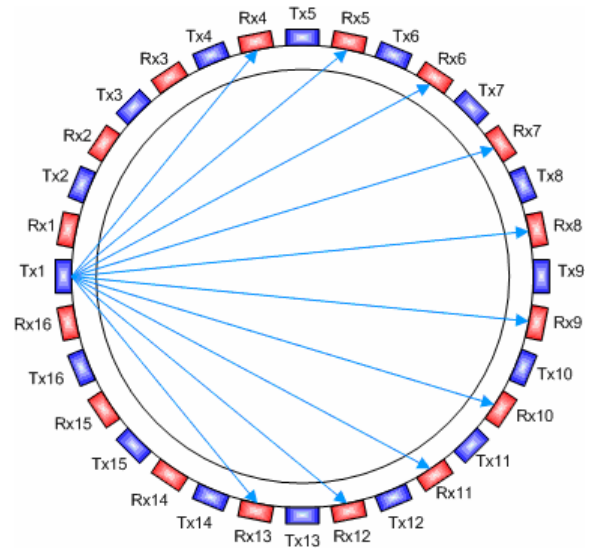


Figure 11: Single scanning geometry.

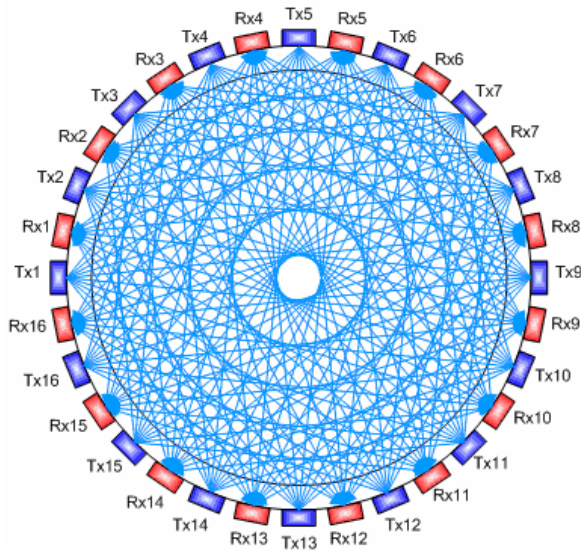


Figure 12: Sixteen scanning geometry.

The dynamic characteristics include the excitation sequence and the synchronization used in data acquisition. The transmitter excitation sequence can be described as follows (by referring to Figure 11 and Figure 12):

1. When data acquisition starts, the first transmitter Tx1 is excited and all receivers will respond to the transmitter pulses.
2. After a time interval (6.667ms @ 150Hz) to allow the reverberation effects of the first pulses to decay, the second transmitter Tx2 is

excited and again all the receivers will detect the transmitted pulses.

3. Next, after the reverberation delay, the third transmitter Tx3 is excited and the transmitted pulses were obtained by the receivers. This sequence is repeated until the last transmitter Tx16 is excited to complete one scanning procedure.

However, improvement on the system can be made by increasing the data acquisition sampling speed which will improve the real-time image performance.

6. Results

The modelling design has been tested with several test objects representing gas bubbles and a stratified flow. The images were reconstructed using the Linear Back Projection Algorithm (LBP) and the Hybrid Binary Reconstruction Algorithm (HBR) [5]. The results are shown in Figure 13.

7. Discussions

The modelling shows that, implementing non-invasive technique require special attention during signal processing. The data obtained by sampling the observation time could be discriminated from the Lamb wave. This method can easily differentiate the liquid and gas phases and therefore reduce the complexity of an ultrasonic tomography system and it leads to high reliability tomography system.

	LBP	HBR
SINGLE GAS HOLDUPS		
DUAL GAS HOLDUPS		

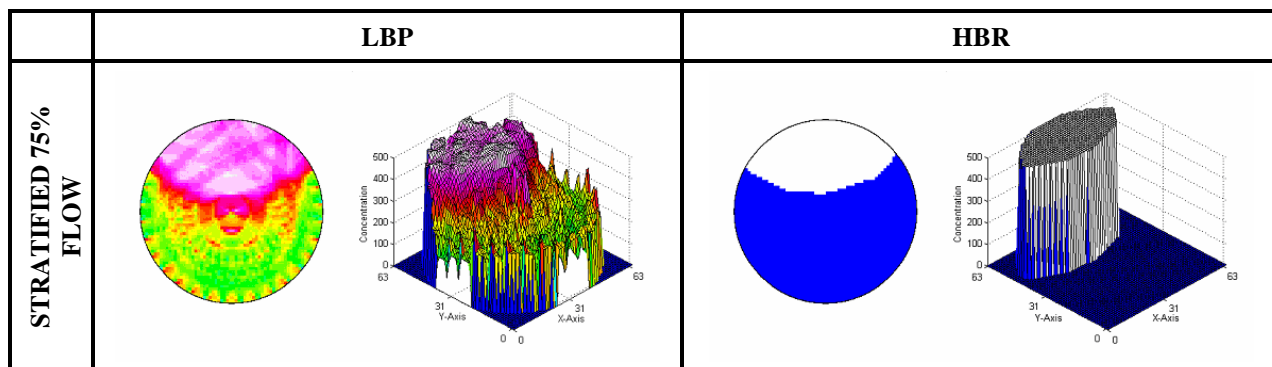


Figure 13: Image Reconstructed using LBP and HBR.

8. References

- [1] R. Abdul Rahim, M. H. Fazalul Rahiman, and K. S. Chan, "Monitoring Liquid/Gas Flow Using Ultrasonic Tomography," in *Proc. 3rd International Symposium on Process Tomography*, Lodz, Poland, 2004, pp. 130-133.
- [2] B. S. Hoyle and L. A. Xu, "Ultrasonic Sensors," in *Process Tomography: Principles, Techniques and Applications*, R. A. Williams and M. S. Beck, Eds. Oxford: Butterworth-Heinemann, 1995, pp. 119-149.
- [3] W. Warsito, M. Ohkawa, N. Kawata, and S. Uchida, "Cross-Sectional Distributions of Gas and Solid Holdups in Slurry Bubble Column Investigated by Ultrasonic Computed Tomography," *Chemical Engineering Science*, vol. 54, pp. 4711-4728, 1999.
- [4] L. Xu, Y. Han, L. A. Xu, and J. Yang, "Application of Ultrasonic Tomography to Monitoring Gas/Liquid Flow," *Chemical Engineering Science*, vol. 52, pp. 2171-2183, 1997.
- [5] M. H. Fazalul Rahiman, "Non-Invasive Imaging of Liquid/Gas Flow Using Ultrasonic Transmission-Mode Tomography," Universiti Teknologi Malaysia, 2005.
- [6] B. S. Hoyle, "Process Tomography Using Ultrasonic Sensors," *Measurement Science Technology*, vol. 7, pp. 272-280, 1996.
- [7] P. I. Moore, G. J. Brown, and B. P. Stimpson, "Ultrasonic Transit-Time Flowmeters Modelled With Theoretical Velocity Profiles: Methodology," *Measurement Science Technology*, vol. 11, pp. 1802-1811, 2000.
- [8] A. Al-Salaymeh and F. Durst, "Development and Testing of a Novel Single-Wire Sensor for Wide Range Flow Velocity Measurements," *Measurement Science Technology*, vol. 15, pp. 777-788, 2004.
- [9] P. Olmos, "Extending the Accuracy of Ultrasonic Level Meters," *Measurement Science Technology*, vol. 13, pp. 598-602, 2002.
- [10] W. Li and B. S. Hoyle, "Ultrasonic Process Tomography Using Multiple Active Sensors for Maximum Real-Time Performance," *Chemical Engineering Science*, vol. 52, pp. 2161-2170, 1997.
- [11] P. Holstein, R. Muller, A. Raabe, M. Barth, D. Mackenzie, K. Arnold, A. Ziemann and M. Schatz, "Acoustical Tomographic Imaging of Flow Field," in *Proc. 3rd World Congress on Industrial Process Tomography*, Banff, Canada, 2003, pp. 318-323.